  Bull. Chem. Soc. Jpn., 60, 4279—4284 (1987)

Reaction of Allyl Phenyl Ether over Various Liquid Metal Catalysts

Sentaro Ozawa,* Yoshiki Sasaki, and Yoshisada Ogino
Department of Chemical Engineering, Faculty of Engineering, Tohoku University, Aramaki-Aoba, Sendai 980
(Received July 8, 1987)

Allyl phenyl ether has been reacted over various kinds of liquid metal catalysts (Sn, Ga, In, Tl, Pb, Cd, Bi, Zn) and without catalysts in the temperature range of 320—500 °C. Phenol (PN), 1,5-hexadiene (HD), benzofuran (BF), and *o*-allylphenol (*o*-AP) together with small amounts of unknown compounds have been found in the condensable products. The results of correlation among the conversion for PN, HD, and BF as well as the results of kinetic simulation of the products distribution have revealed that only the *o*-AP formation is catalyzed by the liquid metal. A clear compensation effect between the frequency factor and the activation energy has been found for the *o*-AP formation reaction, suggesting that a radicalic high energy and high entropy transition state is involved in the catalysis. A good correlation between the methyl group-catalyst metal bond energy and kinetic parameters of the *o*-AP formation reaction has also supported the radicalic transition state model.

Although much information about the catalysis of liquid metals has been accumulated by one of the present authors,[1,2] there remain many problems to be clarified. For instance, characteristics of reactions involving free radicals over liquid metals are not fully investigated. This kind of reaction is interesting not only from the scientific point of view but also from the practical point of view;[3-5] e.g. as model compounds reactions for coal liquefaction and heavy oils up grading reactions.

In the present study, the reaction of allyl phenyl ether which models ether linkages in coal structures has been examined using several liquid metals as catalysts. The experimental results have revealed that the reaction consists of noncatalytic decomposition reactions and a catalytic rearrangement reaction. This reaction scheme has been utilized to derive kinetic equations available for simulating the observed product distribution curves. The purpose of this paper is to report on details regarding the experimental results and to discuss the characteristic features of liquid metal catalysis.

Experimental

Materials. Tin (Sn), indium (In), gallium (Ga), thallium (Tl), cadmium (Cd), lead (Pb), bismuth (Bi), and zinc (Zn) were commercially obtained and used as catalysts in their molten states. Prior to the activity measurement, each catalyst metal was purified by the method reported earlier.[1] Ally phenyl ether (APE) was commercially obtained (reagent grade) and used as a reactant without further purification; benzene was used as a solvent of the reactant (2.5 wt% APE in benzene). Hydrogen was used as a carrier gas of the reactant and as a catalyst purification gas, after a deoxygenation with a Pd-catalyst at 250 °C and a drying with a liquid nitrogen trap.

Procedures. A bubbling type reactor[1,2] made from Pyrex glass was used in the activity measurements. Since details of the experimental method with a reactor of this type have already been reported elsewhere,[1,2] the precedures are only briefly described below.

After purification, the catalyst liquid metal was transferred from the catalyst preparatory tube to the reactor tube through a glass line connecting both tubes under a streaming of purified hydrogen which prevented the catalyst from contamination due to oxidation. Then the reactant solution and hydrogen were fed to the reaction system; the feed rate of the reactant solution was 5.25 $cm^3 h^{-1}$ and that of hydrogen was 82.5 $cm^3 min^{-1}$. The reactant solution was evaporated in a preheater and a gaseous mixture of allyl phenyl ether, benzene, and hydrogen was led to the bottom of the reactor. The mixture was then forced to bubble into the liquid metal catalyst (ca. 10 cm^3) kept at a predetermined reaction temperature. The effluents from the reactor were cooled and condensable materials were separated from gaseous materials. The products, thus obtained, were analyzed by means of a gaschromatography. The instrument used was a Hitachi-163 gaschromatographic apparatus equipped with a capillary column (Hewllet-Packard 19091A-105; 50 m) and a FI detector. The conditions of the analysis were as follows; sample size=1 μl for condensed samples, 1 cm^3 for gaseous samples; injection temperature=260 °C; flow rate=144 $cm^3 min^{-1}$; column temperature=keeping at 50 °C for 9 min followed by a raising at a rate of 10 °C min^{-1}. In addition to the above mentioned analysis, a gas chromatographic mass spectrometry was carried out in identifying important products (JEOL JMS-D300 instrument).

Results and Discussion

Products Distributions. The main products obtained were 1,5-hexadiene (HD), phenol (PN), benzofuran (BF), and *o*-allylphenol (*o*-AP). Methane and a small amount of propene were also found in the gaseous products. A few unknown products were observed. The amounts of these byproducts were estimated by gas chromatography using an averaged calibration curve obtained from the curves of known products. Part of the byproducts probably contain the C_3-group since the ratio of HD/PN was less than 1/2 (mole ratio). Another cause of the deficient HD formation would be polymerization of C_3-radicals; a contaminaion of the outlet of reactor suggested this. Uncertainties due to hydrogenation would be insignificant because the liquid metal little catalyzes the hydrogenation and the residence time is very short. This view is supported by the small amount of observed propene.

The temperature dependences of the above-men-

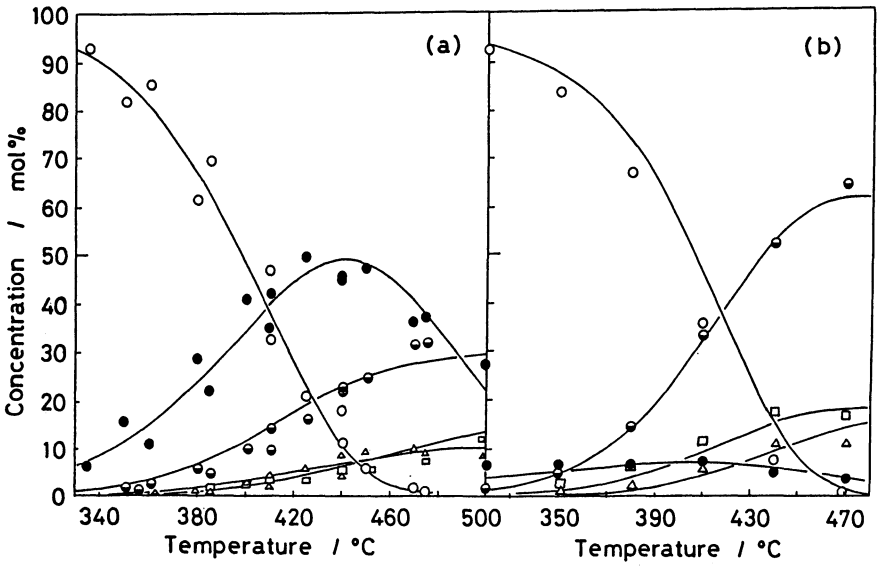

Fig. 1. Products distribution as a function of reaction temperature. (——) Simulation; (a) Sn catalyst; (b) without catalyst; ○: APE, ●: *o*-AP, ◒: PN, □: HD, △: BF.

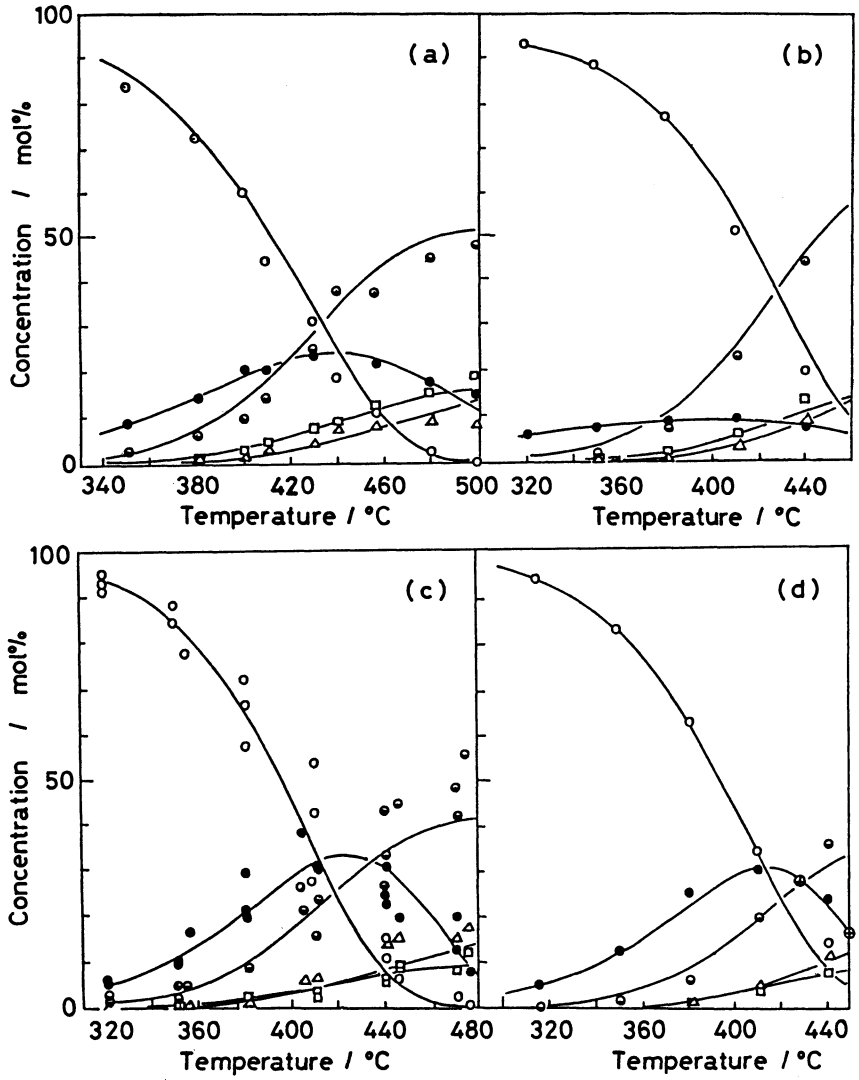

Fig. 2. Products distribution as a function of reaction temperature. (——) Simulation; (a) Pb catalyst, (b) Bi catalyst, (c) Ga catalyst, (d) In catalyst; ○: APE, ●: *o*-AP, ◒: PN, □: HD, △: BF; ⊕: *o*-AP formation activity of Zn catalyst.

tioned liquid products are shown in Figs. 1—3; data points representing concentrations estimated for unknown products were not shown, in order to avoid confusion. The first figure, Fig. 1, shows the two most typical cases observed in the present study. It is seen in Fig. 1 (a) that the reaction over the liquid tin (Sn) catalyst has produced a significant amount of *o*-AP. On the other hand Fig. 1 (b) shows that *o*-AP formation is insignificant and, instead, PN formation is significant in the noncatalytic reaction. This informs us of a difference between the catalytic reaction and the noncatalytic reaction, i.e. the former reaction favors the *o*-AP formation while the latter reaction favors the PN formation. The experimental results shown in Figs. 2 and 3 inform us of an existence of wide differences in the *o*-AP forming activity among the catalyst metals. Concentrations of other products (HD, PN, and BF) also vary upon changing the catalyst metal; however, the extent of variation is smaller compared with that observed for the *o*-AP concentration. This

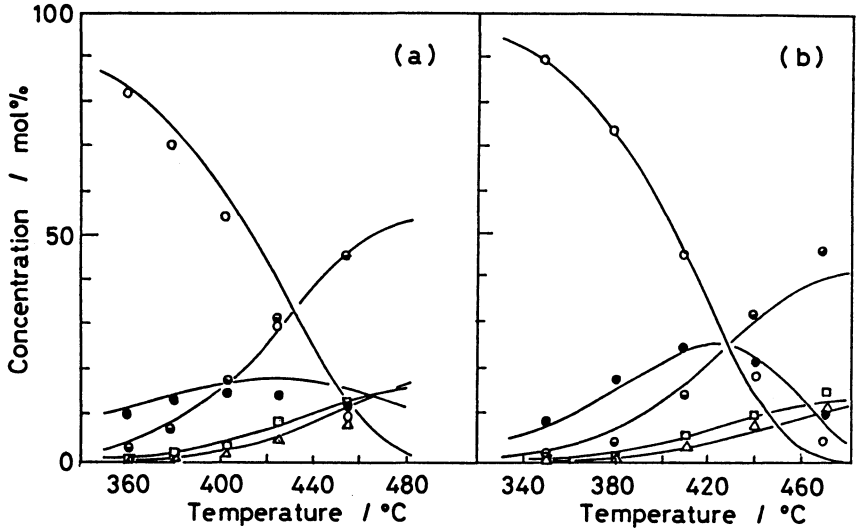

Fig. 3. Products distribution as a function of reaction temperature. (——) Simulation; (a) Cd catalyst, (b) Tl catalyst; ○: APE, ●: *o*-AP, ◒: PN, □: HD, △: BF.

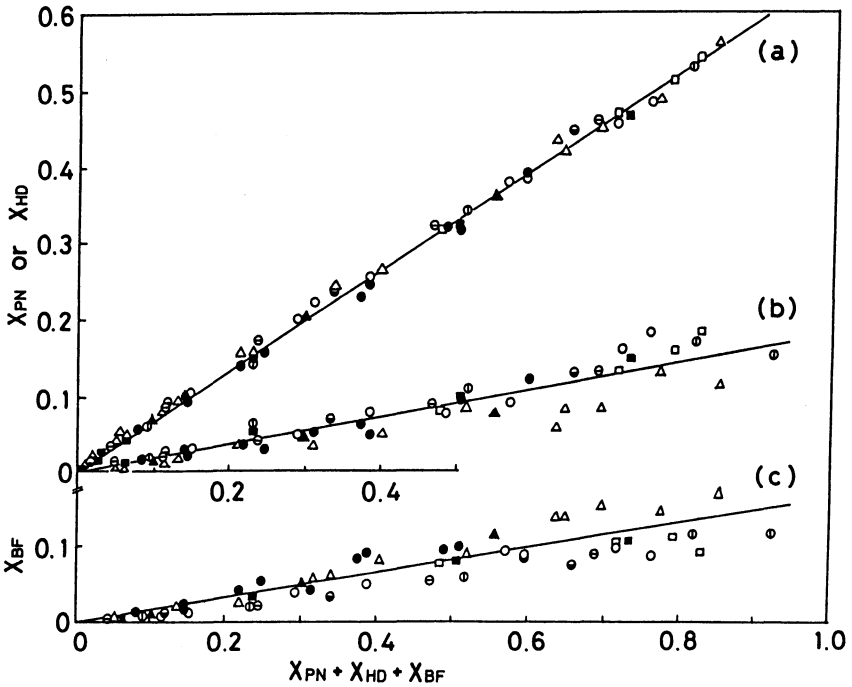

Fig. 4. Linear correlations between the sum of conversions for PN, HD, and BF and the individual conversion for PN, HD, or BF. (a) PN, (b) HD, (c) BF; ○: Pb, ◒: Bi, △: Ga, □: Zn, ●: Sn, ■: Tl, ⊖: Cd, ▲: In, ⊕: without catalyst.

suggests a mechanistic difference between the *o*-AP formation reaction and the other reactions forming HD, PN, and BF.

Relations among Conversions. The relations shown in Fig. 4 (a)—(c) reveal an important aspect of the reaction of allyl phenyl ether (APE). The abscissa of this figure represents the sum of conversions ($\sum X_j$; j=HD, PN, BF) and the ordinate represents the conversion for individual product, i.e. X_{HD}, X_{PN}, or X_{BF}. It can be seen in Fig. 4 (a) that a linear relation exists between $\sum X_j$ and X_{PN}. Furthermore, the straight line represents every data point, irrespective of the catalyst species and conditions used in taking the experimental data; data obtained with different catalysts, data obtained without catalysts, and the data obtained at different temperatures are represented by a single straight line. These facts indicate that the PN formation reaction is essentially noncatalytic, i.e. the catalysts have little affected the PN formation rate. Relations similar to that observed in Fig. 4 (a) can be seen both in Fig. 4 (b) and in Fig. 4 (c), though data points somewhat scatter around the correlation lines. It is possible, therefore, to consider that both the HD formation and BF formation are essentially noncatalytic. The temperature independences of the correlation lines mentioned above suggest that the temperature dependences of X_{HD}, X_{PN}, and X_{BF} are almost identical with each other.

Reaction Scheme and Kinetic Treatments. On the basis of the above-mentioned discussion, the reaction scheme shown in Fig. 5 has been assumed. The reaction scheme consists of five elementary steps. The steps forming HD, PN, and BF are noncatalytic while the step forming *o*-AP is catalytic. A noncatalytic step where *o*-AP decomposes to unknown product (UN) has been added in order to account for the decreasing of the *o*-AP concentration at high temperatures (Figs. 1—3). The symbols k_j (j=1—5) shown in the reaction scheme are the first-order rate constant of the j-th elementary step.

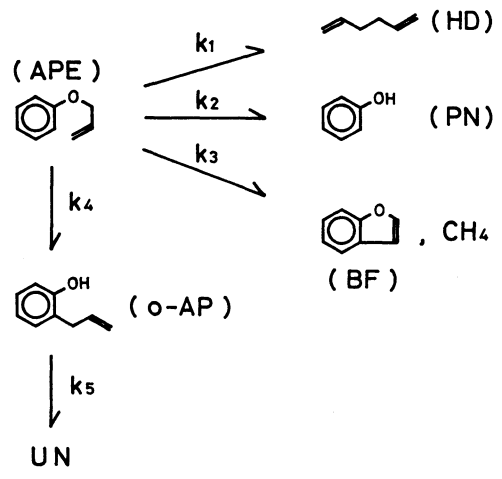

Fig. 5. Reaction scheme of allyl phenyl ether transformation.

If we assume that every step obeys irreversible first-order kinetics, the following relations can easily be derived:

$$1-X_{APE} = \exp(-kt), \quad (1)$$

$$X_{HD} = (k_1/k)[1-\exp(-kt)], \quad (2)$$

$$X_{PN} = (k_2/k)[1-\exp(-kt)], \quad (3)$$

$$X_{BF} = (k_3/k)[1-\exp(-kt)], \quad (4)$$

$$X_{o\text{-}AP} = \exp(-k_5t)[k_4/(k-k_5)][1-\exp(k_5-k)t], \quad (5)$$

where $k=k_1+k_2+k_3+k_4$ and t denotes the reaction period (residence time).

From Eqs. 2—4 we can derive the following relations:

$$X_{HD}/(X_{HD}+X_{PN}+X_{BF}) = k_1/(k_1+k_2+k_3), \quad (6)$$

$$X_{PN}/(X_{HD}+X_{PN}+X_{BF}) = k_2/(k_1+k_2+k_3), \quad (7)$$

$$X_{BF}/(X_{HD}+X_{PN}+X_{BF}) = k_3/(k_1+k_2+k_3). \quad (8)$$

It is evident from these equations that, if activation energies for k_1, k_2, and k_3 are identical with each other, the right hand side of each equation becomes constant and the experimental results shown in Fig. 4 (a)—(c) can be explained. This result indicates that the kinetic treatment mentioned above is promissing. The extent of the constancy of the activation energies will be shown in the following section.

Simulation of Experimental Results. The validity of the reaction scheme and the kinetic treatment mentioned above has been proved by simulating experimentally observed products distribution curves. For this purpose, every rate constants (k_1—k_5) have been converted to the Arrhenius form, i.e. $k_j=a_j\exp(-E_j/RT)$; a_j is the frequecy factor, E_j is the activation energy, R is the gas constant, and T is the absolute temperature. With this expression and with Eqs. 1—5, the experimental results shown in Figs. 1—3 have been simulated and the most probable values for a_j and E_j have been determined; the residence time t has been estimated to be 0.1 s[6] from the reactant flow rate and the reactor volume, and a_j as well as E_j have been determined by trials. The results of simulation are shown in Figs. 1—3 by solid lines and the values of a_j and E_j are summarized in Table 1. The figures show that the experimental results have been well simulated by the calculated lines.

The values of kinetic parameters a_j and E_j (Table 1) deserve special comments. As can be seen in the table, the kinetic parameters (in particular the frequency factor) for the *o*-AP formation reaction, a_4, varies very widely upon changing the catalyst species. On the other hand, the extents of variation of kinetic parameters for other reactions are limited within small ranges compared with that of the *o*-AP formation step. These facts confirm that only the *o*-AP formation step has been catalyzed and the other steps have been little catalyzed by the liquid metal. It must also be pointed out that each value for E_1, E_2, and E_3 does not differ much from the average value of 142 kJ mol^{-1}. The deviations

Table 1. Values of Kinetic Parameters for Different Catalysts and for Noncatalytic Reaction

Catalyst	Frequency factor/s^{-1}					Activation energy/kJ mol^{-1}				
	$a_1/10^{10}$	$a_2/10^{10}$	$a_3/10^{12}$	a_4	$a_5/10^{12}$	E_1	E_2	E_3	E_4	E_5
Pb	1.3	0.8	1.8	2.7×10^5	0.5	135	124	167	65	163
Bi	1.5	1.0	2.0	8.5×10^1	—	135	124	165	24	—
Ga	1.5	6.0	3.0	9.5×10^7	4.0	135	134	165	95	163
Sn	1.3	0.9	2.0	1.8×10^8	0.7	135	126	165	98	162
In	1.5	2.0	2.5	2.2×10^7	0.5	135	128	163	86	146
Cd	1.5	1.1	2.0	5.0×10^3	—	135	126	165	43	—
Tl	1.5	4.5	2.0	3.5×10^7	3.0	134	134	165	91	159
Non	1.1	2.0	1.9	3.7×10^2	—	128	126	163	33	—

of every E_j values (j=1—3) from this average value inform us of the extent of approximation of the constant activation energy, i.e. E_j=constant, discussed in the preceding section.

Catalysis over Liquid Metals. As proved in the above mentioned discussion, only the *o*-AP formation step is regarded as a catalytic reaction. It must be pointed out here that this reaction is a well-known Claisen rearrangement reaction.[7,8] According to literature,[8] the rearrangement proceeds at low temperatures (190—220 °C) without catalysts, though a residence time of several hours is required to obtain a conversion of ca. 85%. Such a homogeneous noncatalytic Claisen rearrangement at low temperatures has been explained in terms of a [3,3]sigmatropic mechanism[8] which requires a highly ordered cyclic transition state. It is unlikely that this mechanism is applicable to explain the results obtained in the present study. The reaction temperature adopted in the present study is much higher and the residence time is much shorter than the respective values mentioned above. Furthermore, the experimental results have shown that the rearrangement is almost inhibited and decompositions prevail in the temperature range studied in this work, if the catalyst is not used. Thus, under the high-temperature conditions adopted in the present study, a homolytic cleavage of the allyl group-oxygen bond is considered to be predominant. It is not unlikely, therefore, that the rearrangement of APE to *o*-AP over the liquid metal proceeds through another mechanism similar to that proposed for the photo-Claisen rearrangement,[9,10] i.e. a radicals recombination mechanism.

In this connection, the relation shown in Fig. 6 reveals an important aspect of the catalysis. The figure shows the existence of a clear compensation effect between the frequency factor a_4 and the activation energy E_4. Qualitatively speaking, this relation indicates that the activation entropy increases with the increase in the activation enthalpy. Thus we can infer from Fig. 6 that a high activation entropy and a high activation enthalpy are associated with the rearrangement reaction over a high activity catalyst, e.g. Sn. In other words, the transition state over the catalyst is expected to have a loosened and unstable structure.

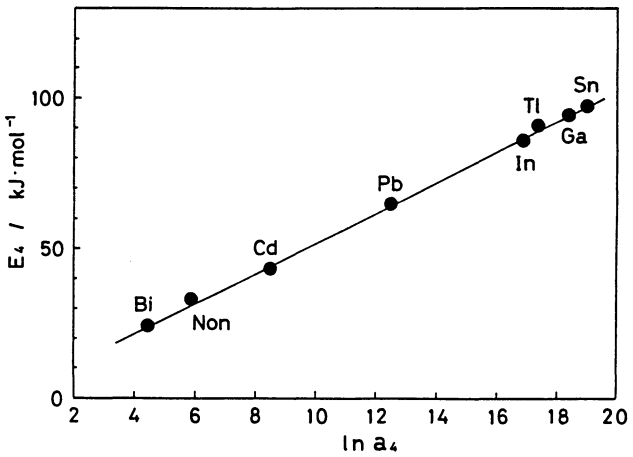

Fig. 6. A compensation effect between the frequency factor and activation energy for the rearrangement reaction.

Thus, a radicalic mechanism in which a phenoxyl radical and an allyl radical pair interaction is involved appears plausible. The cyclic transition state model proposed for the low-temperature homogeneous Claisen rearrangement is unprobable because this model should require a small activation entropy.[8]

If we assume the above-mentioned radicalic mechanism, the result shown in Fig. 6 suggests that the decreasing order of the radical-catalyst interaction energy would be Sn>Ga>Tl>In>Pb>Cd>Bi. This view is indirectly, but strongly, supported by the relation shown in Fig. 7. This figure informs us of that both a_4 and E_4 can be well correlated with the bond energy $Q_{C\text{-}Me}$, the bond energy per one carbon-metal linkage in $(CH_3)_n$-Me (Me=metal, n=an integer).[11-13] It is not unlikely that the $Q_{C\text{-}Me}$ value approximates the interaction energy between the reacting radical and the catalyst metal.

It appears worth reporting that the correlation shown in Fig. 7 enables us to discuss the catalytic activity of liquid zinc (Zn). Since this metal melts at ca. 420 °C, its activity can not be measured at low temperatures and, hence, kinetic parameters for this metal are unknown. It is possible, however, to expect that the activity of Zn would approximately be equal to that of In because $Q_{C\text{-}Zn}$ is 175.7 kJ mol^{-1} which lies

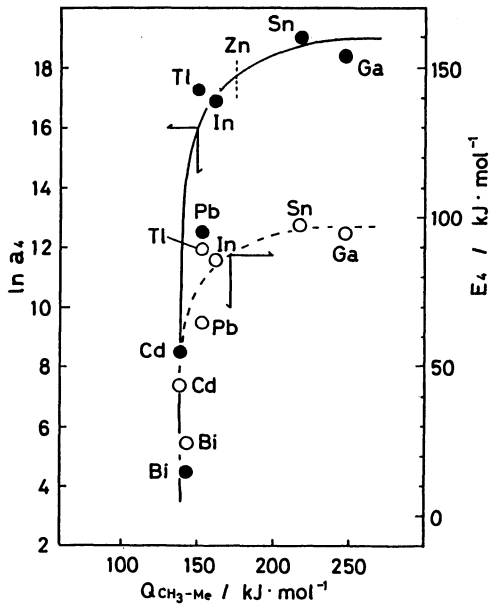

Fig. 7. Correlations between methyl group-metal bond energy and kinetic parameters for the rearrangement reaction. —●—: frequency factor, --○--: activation energy. The bond energy for Tl was taken from CRC "Handbook of Chemistry and Physics," 62nd ed, CRC Press Inc. (1981—1982, F-195. Other values were taken from H. A. Skinner, *Adv. Organomet. Chem.*, **2**, 49 (1964) and "Kagaku Binran; Kisohen II," ed by Chem. Soc. Jpn., Maruzen, Tokyo (1975), pp. 959—978.

close to the value of $Q_{C\text{-}In}$, as we can see in Fig. 7. Indeed, the experimental results shown in Fig. 2 (d;⊕) inform that the catalytic activities observed for Zn at 430 and 455 °C are close to the line representing the *o*-AP formation activity of In.

References

1) Y. Ogino, *Catal. Rev.-Sci. Eng.*, **23**, 505 (1981).

2) Y. Ogino, "Catalysis and Surface Properties of Liquid Metals and Alloys," Marcel Dekker, Inc., New York (1987), pp. 9, 10.

3) D. D. Whitehurst, T. O. Michell, and M. Farcasiu, "Coal Liquefaction," Academic Press, New York (1980), pp. 274—342.

4) L. R. Rudnick and D. Tueting, *Fuel*, **63**, 153 (1984).

5) S. J. Hurff and M. T. Klein, *Ind. Eng. Chem. Fundam.*, **22**, 426 (1983).

6) The residence time t of 0.1 s is not so accurate but this never affects the value of the activation energy obtained. Instead, the error (Δt) in the residence time brings about a shift of logarithm of the frequency factor by $\ln(1+\Delta t/t)$ or ca. $\Delta t/t$ if $-1<\Delta t/t<1$. However the extent of this shift is expected to be almost identical for every catalysts used. Thus the relative magnitudes of frequency factors obtained would not vary. For the understanding of above mentioned description, it must be noted that the following relation has been used in evaluating, for instance, E_1 and a_1;

$$\ln(a_1 t)-E_1/RT= \ln(C_B/C_{A_o})+\ln[\ln(C_{A_o}/C_A)] -\ln[1-(C_A/C_{A_o})].$$

Methods similar to this were used in evaluating other E_j and a_j.

7) D. S. Tarbell, "Organic Reactions," ed by R. Adama, W. E. Bachmann, L. F. Fieser, J. R. Johnson, and H. R. Sryder, John Wiley & Sons, Inc., New York (1944), Vol. II, pp. 1—47.

8) S. A. Rhoads and N. R. Raulins," Organic Reactions," ed by J. E. Baldwin, R. B. Bittman, W. G. Duben, R. F. Heck, A. S. Kende, W. Leimgruber, J. A. Marshall, B. C. McKusick, J. Meinwald, B. M. Trost, and B. Weinstein, John Wiley & Sons., Inc., New York (1975), Vol. XXII, pp. 1—251.

9) G. Koga and N. Kikuchi, *Bull. Chem. Soc. Jpn.*, **41**, 745 (1968).

10) N. Shimamura and A. Sugimori, *Bull. Chem. Soc. Jpn.*, **44**, 281 (1971).

11) H. A. Skinner, *Adv. Organomet. Chem.*, **2**, 49 (1964).

12) "Kagaku Binran; Kiso-hen II," ed by Chem. Soc. Jpn., Maruzen, Tokyo (1975), pp. 959—978.

13) CRC "Handbook of Chemistry and Physics," 62nd ed, CRC Press Inc. (1981—1982), F-195.